

Scotland's Rural College

The feruloyl esterase from *Thermobacillus xylanilyticus* shows broad specificity for processing pre-biotic feruloylated xylooligosaccharides at high temperatures

Garbelotti, Carolina V.; Bulmer, Gregory S.; Ward, Richard J.; van Munster, Jolanda M.

Published in:
Food Chemistry

DOI:
[10.1016/j.foodchem.2022.134939](https://doi.org/10.1016/j.foodchem.2022.134939)

Print publication: 30/03/2023

Document Version
Publisher's PDF, also known as Version of record

[Link to publication](#)

Citation for published version (APA):

Garbelotti, C. V., Bulmer, G. S., Ward, R. J., & van Munster, J. M. (2023). The feruloyl esterase from *Thermobacillus xylanilyticus* shows broad specificity for processing pre-biotic feruloylated xylooligosaccharides at high temperatures. *Food Chemistry*, 405(Pt B), Article 134939. <https://doi.org/10.1016/j.foodchem.2022.134939>

General rights

Copyright and moral rights for the publications made accessible in the public portal are retained by the authors and/or other copyright owners and it is a condition of accessing publications that users recognise and abide by the legal requirements associated with these rights.

- Users may download and print one copy of any publication from the public portal for the purpose of private study or research.
- You may not further distribute the material or use it for any profit-making activity or commercial gain
- You may freely distribute the URL identifying the publication in the public portal ?

Take down policy

If you believe that this document breaches copyright please contact us providing details, and we will remove access to the work immediately and investigate your claim.



The feruloyl esterase from *Thermobacillus xylanilyticus* shows broad specificity for processing pre-biotic feruloylated xylooligosaccharides at high temperatures

Carolina V. Garbelotti^a, Gregory S. Bulmer^b, Richard J. Ward^{a,*}, Jolanda M. van Munster^{b,c,*}

^a Departamento de Química, Faculdade de Filosofia, Ciências e Letras de Ribeirão Preto, Universidade de São Paulo, Ribeirão Preto, SP, CEP 14040-901, Brazil

^b Manchester Institute of Biotechnology (MIB) & School of Natural Sciences, The University of Manchester, 131 Princess Street, Manchester M1 7DN, United Kingdom

^c Scotland's Rural College, West Mains Road, King's Buildings, Edinburgh EH9 3JG, United Kingdom

ARTICLE INFO

Keywords:

Carbohydrate processing
Ferulic acid
Wheat bran
Oligosaccharides
Dietary fibre
Prebiotic

ABSTRACT

Ferulic acid has antioxidant properties of interest to the food industry and can be released from natural plant fibres using feruloyl esterases. Esterases active at high temperatures are highly desirable but currently under-represented. Here we report the biochemical characterization of the feruloyl esterase from *Thermobacillus xylanilyticus*. Specific activity of recombinant Tx-Est1 with ethyl ferulate was $29.2 \pm 2.9 \text{ U mg}^{-1}$, with a catalytic efficiency (K_{cat}/K_m) of $393.7 \pm 9.8 \text{ s}^{-1}\text{mM}^{-1}$. The temperature and pH optima were 60 °C and 7.5, whereby Tx-Est1 retains 70% activity after 25 h at 40 °C. MALDI-TOF MS revealed Tx-EST1 released ferulic acid from xylooligosaccharides with DP4-DP13, and from DP6-8 containing two ferulic acid groups. HPLC demonstrated ferulic acid release from destarched wheat bran was strongly potentiated by co-incubation with xylanase. These properties, especially the high activity at elevated temperatures, suggest Tx-Est1 can be employed for production of high-value compounds from agricultural waste or during plant polysaccharide saccharification.

1. Introduction

The enzymatic treatment of food for modulation of taste, texture and handling properties during processing is a well-established and safe technology that improves food quality for both human and animal consumption (van Boekel et al., 2010). The exceptional regio- and stereospecificity of enzyme catalysis offers the possibility of precise modification of food components on a large scale, and the food industry makes widespread use of glycosyl hydrolases, lipases, proteases and oxidoreductases in a diverse variety of applications (Raveendran et al., 2018). Microbial enzymes are particularly useful to the food industry due to the ease and scalability of production using renewable resources, low environmental impact and their reduced cost (Singh et al., 2016), and the use of both native and recombinant enzymes in food applications is increasing (Trono, 2019).

The hydrolysis of long acyl chains in oils and fats by lipases has been widely exploited to alter the properties of food emulsions (Chandra et al., 2020) and to enhance the taste of dairy products (Jooyandeh et al.,

2009). However, the use of esterases to specifically process short acyl and other common ester-linked food constituents has received less attention. Feruloyl esterase, or ferulic acid esterase (FAE, EC 3.1.1.73), hydrolyses the ester linkage between the ferulic acid (FA, or 4-hydroxy-3-methoxycinnamic acid) and the carbohydrate backbone in branched arabinoxylans and pectins, polysaccharides that are typically found in the cell walls and seed husks of many commelinid plants that are routinely consumed as dietary fibre. Ferulic acid is a bioactive compound, and due to its phenolic nature has been identified as a biological antioxidant that may offer protection against neurodegenerative diseases, thrombosis and cancer and improve glucose uptake as part of diabetes treatment (Nankar et al., 2017). Synergism in intestinal microflora involving FAE producing bacterial strains improve the release of FA from dietary fibre and formation of prebiotic dietary polyphenols (Raveendran et al., 2018), and FAE activity has been shown to influence the probiotic effect of FA release by microorganisms (Russo et al., 2020).

Ferulic acid and many of its derivatives also have antimicrobial

* Corresponding authors at: Departamento de Química, FFCLRP - Universidade de São Paulo, Av. Bandeirantes, 3900, Ribeirão Preto, São Paulo, CEP 14049-901, Brazil (R.J. Ward); Scotland's Rural College, West Mains Road, King's Buildings, Edinburgh EH9 3JG, United Kingdom (J.M. van Munster).

E-mail addresses: carolina.garbelotti@usp.br (C.V. Garbelotti), g.bulmer@mmu.ac.uk (G.S. Bulmer), rjward@ffclrp.usp.br (R.J. Ward), jolanda.van-munster@sruc.ac.uk (J.M. van Munster).

<https://doi.org/10.1016/j.foodchem.2022.134939>

Received 27 April 2022; Received in revised form 7 November 2022; Accepted 9 November 2022

Available online 12 November 2022

0308-8146/© 2022 The Authors. Published by Elsevier Ltd. This is an open access article under the CC BY license (<http://creativecommons.org/licenses/by/4.0/>).

properties, which has led to efforts to develop their use as natural food preservatives (Kumar & Pruthi, 2014) and as a natural cross-linking agent in edible synthetic biofilms for food packaging, thereby providing an antimicrobial and antioxidant coating and reducing the use of non-biodegradable plastic films (Ou et al., 2005). Furthermore, crosslinking of FA and derivatives to form adducts such as 5-5', 8-5', 8-8', and 8-O-4'-diferuloyl linkages (Mathew & Abraham, 2008) between arabinoxylan or pectin polysaccharides in lignocellulose contributes to the chemical resistance of lignocellulose towards enzymatic digestion (Grabber et al., 1998). Treatment of lignocellulose with FAE improves enzymatic saccharification for bioenergy use (Wong, 2006), and enzymatic removal of FA can increase silage digestibility in ruminant feedstocks whilst simultaneously decreasing FA levels to non-toxic levels for rumen microorganisms (Akin et al., 1993). In addition, vanillin and related compounds such as vanillic acid and vanillyl alcohol are high-value natural product derivatives of FA which find applications as flavouring agents in foods and beverages (Koseki et al., 1996).

Due to the increasing interest in FA and its uses, FAEs have attracted attention as valuable biotechnological tools, and based on a wealth of sequence and functional data the FAE enzyme classification system currently includes 13 enzyme subfamilies (Dilokpimol et al., 2016). Although fungi have been the principal focus both for biotechnological applications and as sources of FAEs (Dilokpimol et al., 2018), prokaryotes are a diverse and extensive resource for the discovery of novel enzymes with catalytic and thermostable properties that are compatible with applications in the food industry. The majority of bacterial FAEs studied to date are derived from *Bacillus spp.* and *Lactobacillus spp.* (J. Donaghy et al., 1998) and present low amino acid similarity with the fungal enzymes. Enzyme stability and activity at high temperature is a highly desirable quality for FAE applied in food processes, and these properties are therefore often the focus of engineering or discovery efforts. However, as recently reviewed by (Oliveira et al., 2019), a group of 61 characterised FAE enzymes displayed a mean optimum temperature of 47.5 °C and median of 50 °C, demonstrating that the majority of characterised FAE have relatively low temperature optima. More stable FAE active at high temperature are therefore of interest for the food industry.

A thermostable FAE has previously been described from the Gram-positive bacterium *Thermobacillus xylanilyticus* (Tx-Est1) (Rakotoarivonina et al., 2011), which demonstrates a high optimum catalytic temperature and catalytic profile that is compatible with biotechnological applications. An amino acid sequence-based characterization groups the Tx-Est1 with the CAZyme "Non-Classified" Carbohydrate Esterase Family CEO, however the enzyme uses methyl ferulate or methyl sinapinate as preferred synthetic substrates (Rakotoarivonina et al., 2011) and can be functionally classified with Class A FAEs. Here we aim to assess the potential of the Tx-Est1 for application in the processing of complex food-derived carbohydrates with prebiotic properties such as cinnamoyl-polysaccharides and oligosaccharides. We describe a more detailed biochemical characterization of the enzyme accompanied by an evaluation of its FAE activity against a synthetic substrate and a range of oligosaccharides derived from wheat bran arabinoxylan.

2. Materials and methods

2.1. Coding region synthesis, expression and purification of feruloyl esterase Tx-Est1

The coding region from gene *tx-est1* from *Thermobacillus xylanilyticus* (Genbank GU592999.1) was synthesized and cloned into expression vector pET28a (+) (Novagen, Madison, WI, USA) using restriction enzymes *NdeI* and *HindIII* (New England Biolabs, Ipswich, MA, USA). The vector was transformed to chemically competent *Escherichia coli* BL21 (DE3) Star™ (*E. coli* F' *ompT hsdS_B* (r_B, m_B) *galcdmrne131* (DE3), Thermo Fisher Scientific, Waltham, MA, USA). Transformed cells were

inoculated into 400 mL LB (Lysogeny broth) medium cultures supplemented with kanamycin (50 µg mL⁻¹) at 37 °C, shaken at 200 rpm and the expression of heterologous Tx-Est1 was induced with 0.5 mM of Isopropyl β-D-1-thiogalactopyranoside (IPTG) at OD₆₀₀ 0.6. The produced protein Tx-Est1 includes an N-terminal 6x-His fusion sequence and was purified by immobilized metal affinity chromatography with a nickel-based resin (HisLink, Promega, Madison, WI, USA). After immobilization, the bound protein was washed with buffer A (TRIS 50 mM, NaCl 100 mM, pH 8.0) supplemented with 5, 10 and 40mM imidazole, and eluted in buffer A supplemented with 250 mM imidazole. Purified enzyme was dialyzed against deionized water to remove imidazole and stored at 4 °C prior to use.

2.2. Enzyme activity assays using the synthetic substrate ethyl ferulate

Activity of Tx-Est1 against ethyl ferulate (Sigma-Aldrich, Inc., St. Louis, MO, USA, catalogue number 320617, CAS 4046-02-0) was assessed by spectrophotometric detection of the conversion of the ester to ferulic acid using an adaptation of the methodology reported by Ralet et al., 1994 with methyl ferulate. Ten microlitres of a 0.05 mg mL⁻¹ enzyme solution was incubated with 100 µM ethyl ferulate in McIlvine buffer (citrate-phosphate 0.2 M), and the consumption of the substrate after 2 min reaction was measured by the reduction in A₃₅₀. The low A₃₅₀ of the ferulic acid product as compared the ethyl ferulate (Supplementary Fig. S1A) ensures that measurements at this wavelength are highly sensitive to changes in substrate concentration yet will suffer minimal interference from the increase in the levels of product. Since the A₃₅₀ of ethyl ferulate showed slight alterations with pH, calibration curves were constructed for each buffered solution and at all pH values that were assayed (Supplementary Fig. S1A). The time course of ethyl ferulate consumption monitored at 350 nm showed a linear consumption of substrate over the first 2 mins of the reaction (Supplementary Fig. S1B) confirming that steady state conditions were maintained over this time scale. One enzyme unit (U) was defined as the amount of enzyme that releases 1 µmol of product per min, and specific activity was defined as units per milligram of protein (U mg⁻¹). To determine the optimal pH and temperature, the reaction was performed in McIlvine buffer at pH values ranging from 4.0 to 8.0, and temperatures ranging from 40 to 70 °C, respectively. Thermostability data was produced by incubating the enzyme in aqueous solution at different temperatures (35 to 60 °C) and measuring the activity against ethyl ferulate at determined time intervals (0 to 1800 min or until enzyme had less than 20% of residual activity). All measurements were performed in triplicate and results presented as the mean value with their respective standard deviation.

2.3. Circular dichroism spectroscopy

Thermal denaturation was monitored by far-UVCD using a Jasco J-815 CD Spectropolarimeter (JASCO Corporation, Easton, MD, USA) equipped with a Peltier temperature control using a 1 mm path length quartz cell. Enzyme concentration was 0.14 mg mL⁻¹ solution in water and 0.157 mg mL⁻¹ solution in McIlvine buffer (citrate-phosphate 0.2 M, pH 7.4). The temperature was varied from 20 to 75 °C at a rate of 1 °C min⁻¹. At 5 °C intervals, spectra were recorded using 4 repeated scans over 190 to 260 nm, with a scan speed of 100 nm min⁻¹ and spectral bandwidth of 2 nm. Protein melting temperatures (T_m) were obtained by fitting the measured ellipticity values at 222 nm normalized to protein concentration over the experimental temperature range to the Boltzmann sigmoid equation using Origin (Version 8.5, OriginLab Corporation), assuming a two-state transition (Kumari et al., 2011).

2.4. Differential scanning calorimetry

Differential scanning calorimetry (DSC) experiments were performed on a Nano-DSC II (TA instruments, Newcastle, DE, USA). The enzyme

concentration was 1.05 mg mL⁻¹ either in deionized water, McIlvaine buffer (citrate–phosphate 0.2 M, pH 7.4) or in the presence of 20 mM ethyl ferulate in buffer. Heating scans were recorded from 10 to 100 °C at a rate of 1.0 °C min⁻¹. Control scans in all experiments used the same solutions without protein. Protein unfolding or melting temperatures (T_m) for each condition were estimated from the maximum of the transition peaks and unfolding enthalpies were calculated by integrating the area under the transition peaks using NanoAnalyze™ software supplied by the manufacturer (TA instruments, Newcastle, DE, USA).

2.5. Processing of sugar cane

Sugar cane *Saccharum* hybrid cultivar SP80-3280 (Centro de Tecnologia Canavieira, Piracicaba, SP, Brazil) was processed as described previously (de Souza et al., 2012). Briefly, sugar cane culms were harvested and dried at 60 °C for 48 h and milled to 20 mesh particles. The resulting powder was subjected to six extractions with 80% (v/v) ethanol and a loading of 50 mL g⁻¹(v_{ethanol}/g_{biomass}) at 80 °C for 20 min. The resulting alcohol insoluble residue (AIR) was washed with deionized water and dried at 60 °C for 24 h. The AIR fraction was treated twice with ammonium oxalate 0.5 M (pH 7.0) and a loading of 50 mL g⁻¹ at 80 °C for 3 h each with stirring. The oxalate-extracted solid was recovered by filtration and extracted with 40 mL g⁻¹ of 3% (m/v) sodium chlorite in 0.3% (v/v) acetic acid at room temperature for 1 h. The chlorite-extracted cell wall was then filtrated from the solution, thoroughly washed with deionized water, and dried at 60 °C for 24 h.

2.6. Production of oligosaccharide enzyme substrates

Commercial wheat bran (Holland & Barrett, Nuneaton, Warwickshire, UK) was ground to a powder with pestle and mortar. The ground material was destarched by incubation of 39 g of the powder in 500 mL of 50 mM phosphate buffer pH 6.5 containing 3.9 mg (~2000 U) α-amylase from *Bacillus licheniformis* (Termamyl 120™, Sigma-Aldrich, Inc., St. Louis, MO, USA, catalogue number A3403, 9000–85-5) for a final concentration of 100 µg (~50 U) amylase/g bran. After 30 min incubation at 80 °C, no starch was detectable with the Lugoliodine test (Cochran et al., 2008). The powder suspension was centrifuged for 10 min at 4000g, washed with an equal volume of deionized water and dried for 16 h at 50 °C, to yield 22.4 g of destarched material.

Ten grams of destarched bran powder was incubated with 0.5 g Driselase (Sigma-Aldrich, Inc., St. Louis, MO, USA – catalogue number D9515, CAS 85186–71-6), containing ~ 50 U of cellulase and ~ 5 U of laminarase, in 1 L of deionized water at 35 °C with stirring at 100 rpm. In a separate reaction, 10 g of the destarched bran powder was incubated with 2 g (~5000 U) of the xylanase from *Thermomyces lanuginosus* (Sigma-Aldrich, Inc., St. Louis, MO, USA, catalogue number X2753, CAS 37278–89-0) in 1 L of 20 mM phosphate buffer pH 7, 35 °C at 35 °C with stirring at 100 rpm. This xylanase releases a pentasaccharide end-product containing an α-1,3-linked arabinose decoration at the pre-terminal non-reducing end xylose (β-D-Xylp-(1–4)-[α-L-Araf-(1–3)]-β-D-Xylp-(1–4)-β-D-Xylp-(1–4)-β-D-Xylp)(Lama et al., 2014)(Biely et al., 2016). After 24 h, the incubations were heated to 100 °C to inactivate the enzymes, and the treated bran powder was separated from the supernatant by centrifugation (10 min at 4000g). The solid bran residue was dried for 16 h at 50 °C, to yield 6.07 and 6.76 g from Driselase and Xylanase treatments, respectively, indicating solubilisation of 39 % and 32 % of the starting material.

Oligosaccharides containing aromatic residues were captured from the supernatant of the enzyme incubations with approximately 10 mL of Amberlite® XAD4 resin (20–60 mesh, Sigma-Aldrich, Inc., St. Louis, MO, USA, catalogue number XAD4, CAS 37380–42-0), washed with 50 mL of deionized water, and eluted with 50 % ethanol and 90 % ethanol. Driselase-derived oligosaccharides were obtained as two pools of 233 mg and 166 mg, and xylanase-derived oligosaccharides as a single pool of 234 mg. The oligosaccharide pools were fractionated with a fine-bead

Bio-Gel P2 (Bio-Rad Laboratories, Inc., Hercules, CA, USA, catalogue number 1504118, CAS 39454–59-6) column (1.5 × 75 cm) at room temperature, eluted with deionized water at 0.5 mL min⁻¹. Fractions of 2–5 mL volume were collected, and an aliquot was analysed by MALDI-TOF mass spectrometry (MS). Fractions from identical enzyme treatments and with similar mass-profiles were pooled and freeze dried for analysis by MALDI-TOF MS and NMR. Based on results of this analysis, only non-redundant fractions were subsequently used for further experiments and analysis.

2.7. NMR analysis of oligosaccharides

Oligosaccharide fractions were dissolved in 650 µL deuterium oxide (Sigma-Aldrich) and analysed by NMR spectroscopy. A Bruker Advance 400 NMR spectrometer (Bruker Nano GmbH, Berlin, Germany), operating at 400.13 MHz and 298.1 K, was used to record ¹H and ¹³C NMR spectra. ¹H NMR spectra were recorded with 30-degree pulses, a data acquisition time of 4.09 s and a relaxation delay of 1 s, with spectral width of 20.03 ppm. Raw spectra were subject to Fourier transform, corrected for baseline and integrated using Bruker TopSpin® software (Bruker Nano GmbH, Berlin, Germany). Spectra were approximately referenced using the deuterium lock, followed by subsequent accurate referencing in the ¹H-dimension by setting the reducing end α-xylose resonance to 5.184 ppm (generating chemical shifts equivalent to those referenced relative to internal acetone (2.225 ppm))(Kormelink et al., 1993; van Munster et al., 2017). Data collection in 2D ¹H-¹³C-HSQC (Heteronuclear Single Quantum Coherence Spectroscopy) NMR experiments used the Bruker pulse program hsqcedetgpsisp2.3 (Bruker Nano GmbH, Berlin, Germany), which enables multiplicity edited HSQC using echo/antiecho detection and gradient pulses. Spectral assignment was based on matching the 1D and 2D data with previous literature reports for esterified and non-esterified arabinoxylan oligosaccharides (Bunzel et al., 2002; Hoffmann et al., 1991; Kormelink et al., 1993; Lequart et al., 1999; Schendel et al., 2015).

2.8. Enzyme activity assays on oligosaccharides and polymeric natural substrates

Oligosaccharides at a concentration of 0.3 mg mL⁻¹ were incubated with 0.1 mg mL⁻¹ recombinant Tx-Est1 (5.8 U) in 50 mM citrate–phosphate buffer pH 6.5 at 60 °C for 30 min. Substrates and reaction products were analysed using MALDI-TOF Mass Spectrometry as described in section 2.9. Polymeric substrates were incubated at 1 w/v with 0.1 mg mL⁻¹ Tx-Est1 (5.8 U), 50 mM citrate–phosphate buffer pH 6.5 at 60 °C for 16 h. Substrates used were: chlorite extracted sugar cane, ethanol extracted sugar cane, wheat bran, wheat straw, acid debranched arabinoxylan (Wheat Flour; 26% arabinose, Megazyme, Bray, Co. Wicklow, Ireland, catalogue number P-ADWAX22), Arabinoxylan (Arabinoxylan (Wheat Flour; Medium Viscosity), Megazyme, Bray, Co. Wicklow, Ireland, catalogue number P-WAXYM) and Arabinoxylan (Wheat Flour; Insoluble, Megazyme, Bray, Co. Wicklow, Ireland, catalogue number P-WAXYI). Reactions co-incubated with *T. lanuginosus* endo-xylanase (Sigma-Aldrich, Inc., St. Louis, MO, USA, catalogue number X2753, CAS 37278–89-0) at a final concentration of 8 mg mL⁻¹ (20,000 U mL⁻¹). Following filtration, all samples were analysed by HPLC as described in section 2.10.

2.9. MALDI-TOF mass spectrometry

Reaction mixtures (0.5 µL) were spotted on target plates, then mixed with 0.5 µL of a 15 mg mL⁻¹ super-DHB (Sigma-Aldrich, catalogue number 50862, CAS 63542–76-7) solution in 50% acetonitrile + 0.1% TFA and dried at ambient temperature. The product was analysed in positive mode on a Bruker Ultraflex (Bruker Nano GmbH, Berlin, Germany) or Autoflex III MALDI-TOF (Bruker Nano GmbH, Berlin, Germany) instrument using the following parameters: laser intensity 40%,

matrix suppression less than 300 Da, reflector intensity 3.2x, detection range 400 to 1900 m/z .

2.10. HPLC of enzyme reaction products

Reverse Phase HPLC was carried out on an Agilent 1260 Infinity II Series system (Agilent Technologies, Santa Clara, CA, USA) equipped with the G1379A degasser, G1312A binary pump, G1316A temperature-controlled compartment and a diode array detector accessories. A Kinetex® 5 μm , C18 100 Å, 50 × 2.1 mm column (Phenomenex, Torrance, CA, USA) was used as a stationary phase, and mobile phase A: Water + 0.1% trifluoroacetic acid and mobile phase B: Acetonitrile + 0.1% trifluoroacetic acid. The flow rate was 0.6 $\text{mL}\cdot\text{min}^{-1}$ with elution following an isocratic gradient 100% A (0–5 min), isocratic 20% B, 5–15 min linear gradient 20–80% B, 15–25 min isocratic 20% B.

3. Results and discussion

3.1. Optimal reaction conditions and kinetic characterisation of Tx-Est1

The Tx-Est1 from *Thermobacillus xylanilyticus* was successfully expressed as an N-terminal 6xHis fusion protein from a pET28a-based construct in *E. coli*. After purification of Tx-Est1 to homogeneity by nickel affinity chromatography (Supplementary Figure S2), the enzyme

was obtained with a final yield of 5 $\text{mg}\cdot\text{L}^{-1}$ culture. Activity of the Tx-Est1 against the synthetic substrate ethylferulate exhibited a specific activity of $29.2 \pm 2.9 \text{ U mg}^{-1}$, a K_M of $0.09 \pm 0.02 \text{ mM}$ (Fig. 1A) and catalytic efficiency (K_{cat}/K_M) $393.7 \pm 9.8 \text{ s}^{-1}\text{mM}^{-1}$. The K_M of the enzyme against ethyl ferulate is similar to that previously reported for methyl ferulate (0.11 mM), methyl-sinapinate (0.10 mM) and lower than that reported for methyl-*p*-coumarate (1.28 mM) (Rakotoarivonina et al., 2011). In addition, Tx-Est1 presented a higher catalytic efficiency against ethyl ferulate, with values 3, 2, 43 and 3-fold from previously reported for the same enzyme against methyl ferulate, methyl-sinapinate, methyl-*p*-coumarate and 4-nitrophenol (*p*NP)-acetate, respectively, indicating it is a better substrate than those previously assayed (Supplementary Table S1). In combination with a previously reported capacity to release diferulate (mainly 5-5' diferulate and 8-O-4 diferulate) from wheat straw (Rakotoarivonina et al., 2011), the catalytic properties identified here place the Tx-Est1 in the Class A FAEs following the functional ABCD classification system (Crepin et al., 2003), which is still the preferred nomenclature for bacterial FAEs since the bacterial enzymes are currently not included in the sequence-based FAE sub-family classification system.

Relatively little information describing the catalytic properties of bacterial FAEs is available in the literature and the diversity of substrates and lack of some catalytic parameters complicates direct comparisons between the previously reported activities of feruloyl esterases.

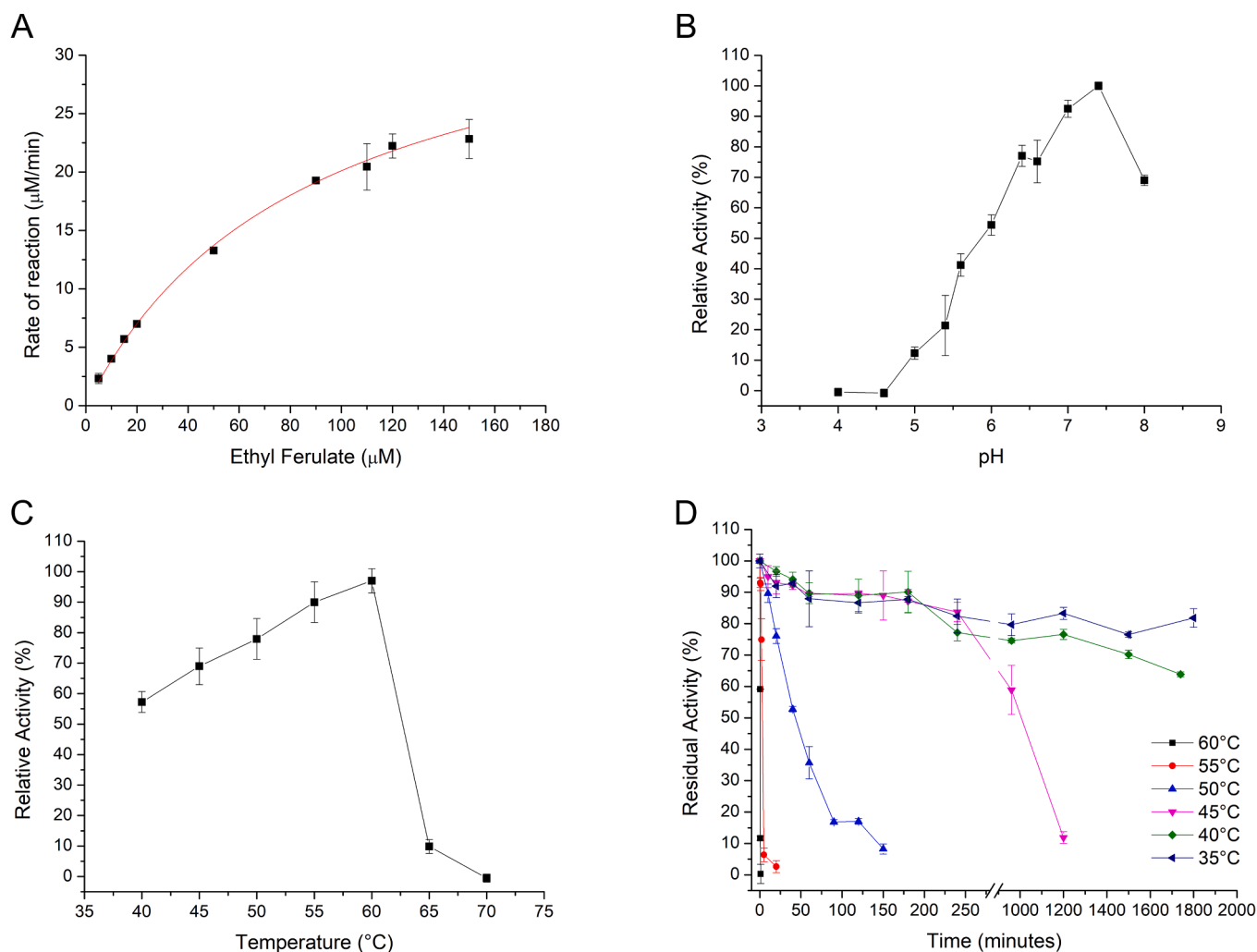


Fig. 1. Biochemical characterisation of Tx-Est1 activity against ethyl ferulate. **A.** The effect of ethyl ferulate concentration on catalytic rate follows Michaelis-Menten kinetics (best fit to the experimental data shown as the red line). Determination of the optimum catalytic pH (**B**), optimum catalytic temperature (**C**) and thermal stability (**D**). See materials and methods section for further experimental details.

However, according to information available in the BRENDA database (Supplementary Table S2), type A FAE from *Thermoanaerobacter tengcongensis* presented similar K_M values of for methyl ferulate, methyl-sinapinate and methyl-*p*-coumarate, but with much lower specific activities (50-fold lower for methyl ferulate and 10-fold lower for the methyl-sinapinate and methyl-*p*-coumarate substrates) and almost 5-fold higher against *p*NP acetate (Abokitse et al., 2010). Unidentified-type FAE from *Clostridium stercorarium*, on the other hand, showed specific activities 3-fold higher against ethyl and methyl ferulate and 30-fold higher against methyl coumarate (J. A. Donaghy et al., 2000), while the specific activity of *Butyrivibrio proteoclasticus* FAE against ethyl ferulate was reported to be of the same order as the Tx-Est1 (Goldstone et al., 2010) but, mostly, specific activities reported for bacterial FAEs are lower than those observed here, considering the same substrates.

Since the Tx-Est1 presents the highest catalytic efficiency against ethyl ferulate, the effect of reaction conditions on the activity of Tx-Est1 towards this substrate was investigated. The enzyme was found to have optimal activity at pH 7.4 (Fig. 1B) and 60 °C (Fig. 1C), while more than 50% of activity was maintained over the pH range 6.0–8.0 and the temperature range 40–60 °C (Fig. 1D). The protein exhibited high stability at temperatures below 45 °C in aqueous solution, retaining more than 70% activity after 25 h and over 80% activity after a week at room temperature (between 20 and 30 °C) or after 6 months at 4 °C (data not shown). The optimal catalytic temperature at 60 °C, but lower stability at 50–60 °C in aqueous solution is explained by the increased structural stability in the presence of substrate, which is consistent with the results of the CD and DSC experiments in which the denaturation temperature increased from 54 °C in aqueous solution to 60 and 63 °C in the presence of reaction buffer and substrate, respectively (Supplementary Figure S3 and Supplementary Table S3). The buffer phosphate/citrate-based buffer used in the activity assays may also result in a lower energy protein conformation stabilizes external residues, also maintaining the pH constant, and the presence of substrate probably causes change to a lower energy conformation (Gianfreda & Scarfi, 1991). However, further structural studies are necessary to confirm such hypothesis.

3.2. Production and characterisation of feruloyl arabinoxylan oligosaccharides

To assess the catalytic capacity of Tx-Est1, activity was tested against more complex and natural substrates. The enzyme was previously shown to be active against feruloylated arabinoxylotetraose (Rakotoarivonina et al., 2011), XFAXX, from wheat bran (xylp- β 1,4-[5-O-FE-Araf- α 1,3]-xylp- β 1,4-xylp- β 1,4-xylp), which contains a ferulated arabinose decorating the second xylose from the non-reducing end (Lequart et al., 1999; Rémond et al., 2008). Here, a panel of cinnamoyl oligosaccharide substrates was prepared by enzymatic digestion of destarched wheat bran followed by chromatography-based fractionation (Bunzel et al., 2002; Schendel et al., 2015). Results for 1D ^1H and 2D ^1H - ^{13}C HSQC

NMR analyses of this panel of oligosaccharides (Table 1, Supplementary Table S4) indicates that each fraction contains an ensemble of oligosaccharides with xylopyranose backbones, and includes fractions containing single α -1,3-linked and/or double α -1,2/ α -1,3-linked arabinofuranose decorations. For all fractions, the presence of ferulic acid was observed, as indicated by the diagnostic signals of C7/H7, C8/H8 and OMe groups (Supplementary Table S4). The proportion of decorated arabinoses calculated from the Araf-C1 associated ^1H signal intensity as a proportion of the FA-derived aromatic ^1H signal, varied between 8 and 104% (Table 1). For the samples with an esterification ratio of greater than 0.2, arabinose-esterification with ferulic acid was confirmed in the HSQC by the diagnostic Araf-C5/H5 signals. Fractions JvM006 and JvM017 represent the most defined substrates, which have 1 and 2 main esterified Araf environments, respectively. As expected after GH11 digestion (Biely et al., 2016), the NMR signals for JvM017 include those corresponding with the presence of esterified oligosaccharide XFAXX (Lequart et al., 1999).

3.3. Broad substrate usage of Tx-Est1 on feruloyl oligosaccharides

The MALDI-TOF analysis of the fractions revealed a variety of ferulic acid-decorated oligosaccharides ranging from degree of polymerisation (DP) 4 – DP 13 (Table 1, Fig. 2 and Supplementary Figures S4–10), in addition to non-decorated oligosaccharides in selected fractions. Additionally, fraction JvM017 (Table 1, Supplementary Figure S11) contained oligosaccharides of DP6, DP7 and DP8 with two ferulic acid groups. The observed *m/z* and Araf decoration ratio suggest that these oligosaccharides contain two esterified Araf each rather than diferulates, but it should be noted that many resonances in the aromatic region of the NMR spectra of these fractions could not be assigned. Incubation of the ferulated xylooligosaccharides with Tx-Est1 revealed enzyme activity against all esterified substrates, with signals corresponding to the ferulic acid-esterified oligosaccharides no longer observed after 30 min incubation. Interestingly, the Tx-Est1 showed catalytic capacity against all the ferulated oligosaccharides including those with additional mono- and di-Araf substitutions, thus indicating that this enzyme accommodates a wide range of substituted soluble substrates without experiencing steric hindrance.

3.4. Activity of Tx-Est1 against complex plant polysaccharides

The activity of Tx-Est1 was assessed against a variety of complex plant polysaccharides and cell wall lignocellulosic material to evaluate its utility in the processing of food ingredients and agricultural waste streams. Release of FA was detected after incubation of the Tx-Est1 with insoluble wheat arabinoxylan (Supplementary Figure S12) and acid-debranched wheat arabinoxylan (Supplementary Figure S13). In contrast, no activity was observed after incubation with medium viscosity wheat arabinoxylan or against wheat straw or chlorite treated

Table 1

Summary of the composition of oligosaccharide fractions as determined by NMR and MALDI-TOF MS. All oligosaccharide fractions can act as substrates for Tx-Est1 as indicated in the final column. Abbreviations indicated as, DP; degree of polymerisation, NA; not observed, FA; ferulic acid, Araf; arabinofuranoside, Araf-s3 and Araf-d2,3 refer to single and double substitution of the xylose with α -1,2 and/or α -1,3-linked Araf.

Oligo-saccharide fraction	Identified decorations (NMR)			Esterification Araf-FA/Araf	(DP MALDI-TOF MS)			Tx-Est1 substrate
	Araf-s3	Araf-d2,3	Araf-FA		DP	DP-FA	DP-2FA	
JvM001	NA	yes	yes	0.1	5–7	7–10	NA	yes
JvM002	NA	yes	yes	0.1	6–9	9–12	NA	yes
JvM003	NA	NA	yes	0.2	NA	4–8	NA	yes
JvM005	NA	NA	yes	0.7	NA	4–6	NA	yes
JvM006	NA	NA	yes	1.0	NA	4–5	NA	yes
JvM010	yes	yes	yes	0.1	7–10	10–13	NA	yes
JvM012	yes	yes	yes	0.1	6	4–10	NA	yes
JvM013	yes	NA	yes	0.2	NA	7–9	NA	yes
JvM014	NA	NA	yes	0.7	NA	5–8	NA	yes
JvM017	NA	NA	yes	1.0	NA	4–5	6–8	yes

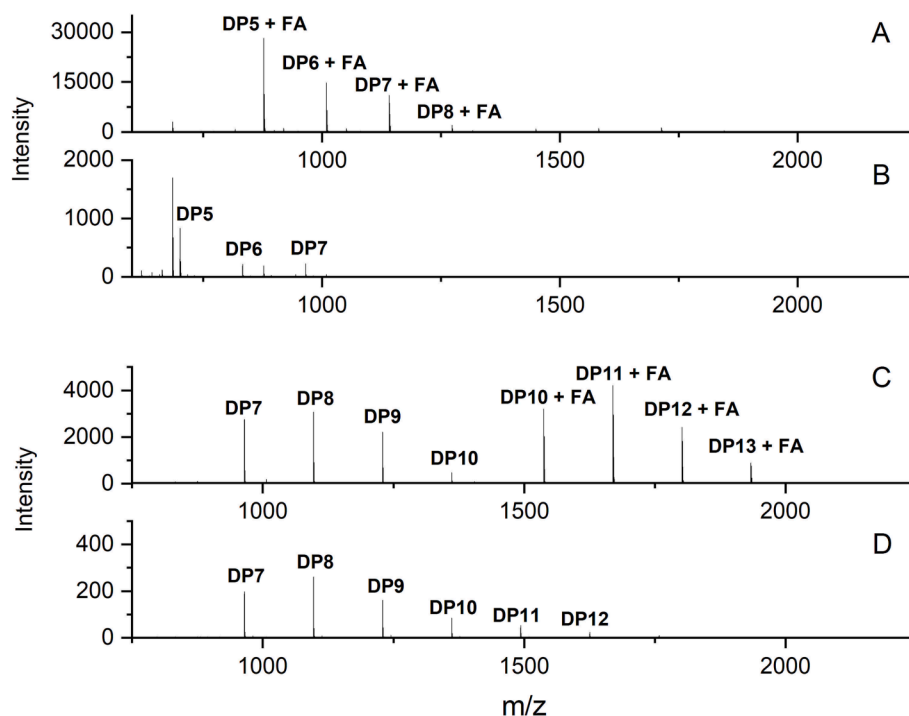


Fig. 2. MALDI-TOF MS spectra of oligosaccharide fractions JvM014 (A,B) and JvM010 (C,D) before (A/C) and after incubation (B/D) with Tx-Est1. Reactions performed in 50 mM pH 6.5 citric acid-phosphate buffer at 60 °C for 30 min. Degree of polymerisation (DP) as indicated, FA, ferulic acid.

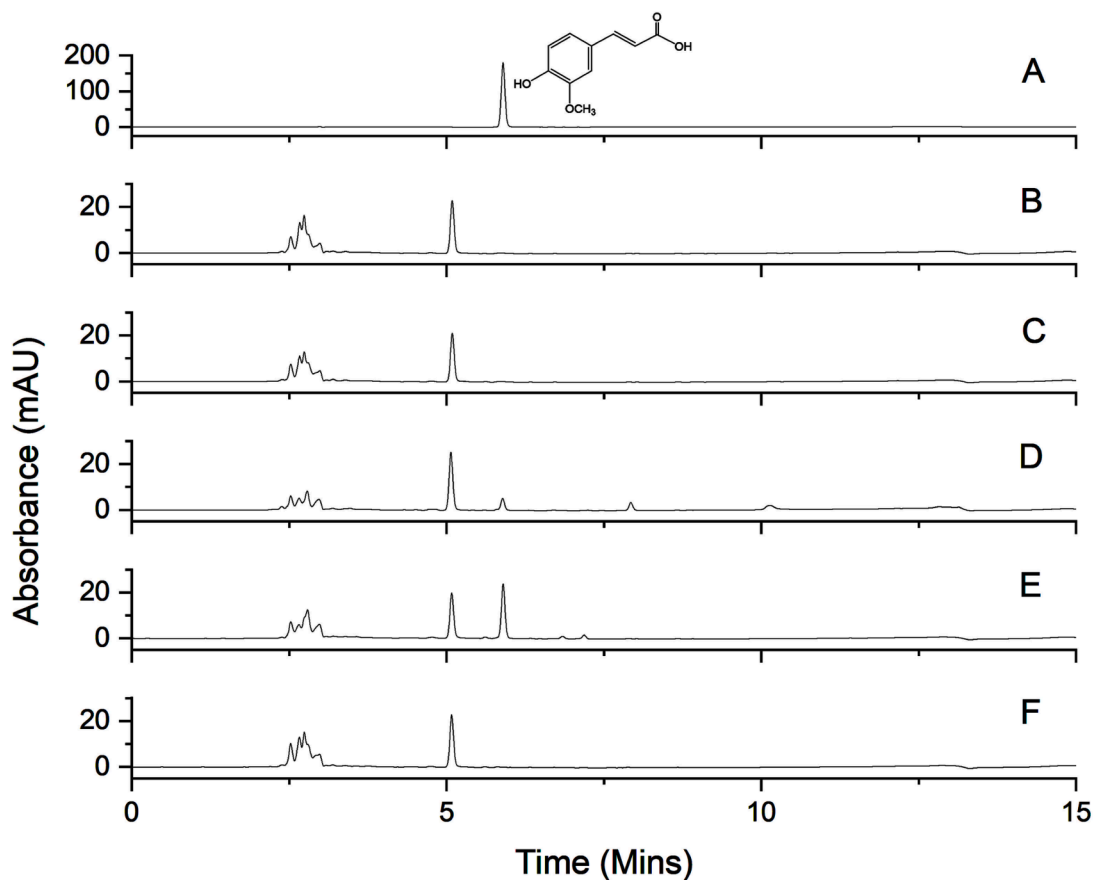


Fig. 3. HPLC profiles of Tx-Est1 against wheat bran. **A** Ferulic Acid 0.5 mM (control). **B** Wheat Bran 1% (w/v) negative control. **C** Wheat Bran 1% (w/v) incubated with *T. lanuginosus* xylanase. **D** Wheat Bran 1% (w/v) incubated with TxEst1. **E** Wheat Bran 1% (w/v) co-incubated with TxEst1 and *T. lanuginosus* xylanase. **F** Wheat Bran 1% (w/v) co-incubated with denatured TxEst1 and *T. lanuginosus* xylanase.

sugarcane. Ferulic acid release was also detected from incubation of wheat bran with active Tx-Est1 ($67 \mu\text{g g}^{-1}$ wheat bran, Fig. 3D), whilst co-incubation with a GH11 xylanase (Fig. 3E) revealed a substantial increase in ferulic acid release (1.0 mg g^{-1} wheat bran) thus suggesting synergism between the Tx-Est1 and GH11 enzymes. Incubation of wheat bran with either xylanase alone (Fig. 3C), or with a combination of xylanase and heat-inactivated Tx-Est1 (Fig. 3F) resulted in no detectable ferulic acid release. Addition of the digestive enzyme mixture Driselase also increased the level of ferulic acid released by Tx-Est1 (1.3 mg g^{-1} wheat bran), but in contrast to previous reports (Kroon et al., 1999) the Driselase alone displayed esterase activity (1.0 mg g^{-1} wheat bran).

These results indicate that the catalytic activity of the Tx-Est1 feruloyl esterase can release ferulic acid directly from the complex matrix of cell wall polymers of wheat bran. Furthermore, in addition to the activity against free oligosaccharides as demonstrated by the mass spectrometry data (Fig. 2), the feruloyl esterase activity is potentiated by xylanases that release a range of ferulated oligosaccharides. This suggests that the activity of Tx-Est1 on the complex cell wall matrices is limited by access to its substrate. This idea is further supported by the differences in the lignin content of the substrates tested here. The sugar cane (bagasse), wheat straw, and wheat bran have been reported to contain 25–32%, 21%, and 3% lignin, respectively (Lequart et al., 1999; Zeng et al., 2014), and it is noteworthy that the Tx-Est1 released the highest levels of ferulic acid from the substrate with the lowest lignin content. Wheat straw and wheat bran are reported to have similar ferulic acid content (Lequart et al., 1999; Barberousse et al., 2008) and the level of ferulic acid in each of these substrates is therefore not expected to contribute to the observed difference.

4. Conclusions

The bioactivities of ferulic acid, coupled with its antioxidant and preservative capabilities, makes it an important ingredient for the food industry. Enzymatic, greener and more cost-effective routes for its production are therefore of great interest for the human and animal feed industries seeking to utilize this compound in their products. In this study, we have expressed heterologous Tx-Est1 feruloyl esterase at 5 mg L^{-1} , and evaluated its catalytic activity against ethyl feruoylate, a range of feruoylated xylooligosaccharides and treated lignocellulose derived from agricultural by-products. The enzyme promoted the removal of all ferulate groups from xylooligosaccharides varying in length from 4 to 13 DP, and in addition could liberate $67 \mu\text{g g}^{-1}$ of ferulic acid from wheat bran. When utilised with a commercially available xylanase, the ferulic acid release showed a 15-fold increase (1 mg g^{-1}) in comparison to Tx-Est1 alone and highlights the synergism between this esterase and other proteins involved in the deconstruction of plant polysaccharides. The good initial expression levels and excellent protein stability, combined with the relatively high optimum temperature for activity, suggests that Tx-Est1 may be amenable to the production scale-up that would be required for eventual large-scale applications. Our data suggests Tx-Est1 can be employed for the production of a high-value compound from agricultural waste streams or as part of the saccharification process of complex, heterogeneous plant polysaccharides.

CRedit authorship contribution statement

Carolina V. Garbelotti: Investigation, Methodology, Visualization, Writing – original draft. **Gregory S. Bulmer:** Investigation, Methodology, Visualization, Writing – original draft. **Richard J. Ward:** Conceptualization, Funding acquisition, Methodology, Supervision, Writing – original draft, Writing – review & editing. **Jolanda M. van Munster:** Conceptualization, Funding acquisition, Methodology, Supervision, Writing – original draft, Writing – review & editing.

Declaration of Competing Interest

The authors declare that they have no known competing financial interests or personal relationships that could have appeared to influence the work reported in this paper.

Data availability

Data will be made available on request.

Acknowledgments

This study was funded by the BBSRC via BB/P011462/1 (JvM), FAPESP-SPRINT research grant 2018/14030-2 (RJW, JvM), FAPESP doctorate fellowship 2018/25664-2 (CVG), the National Institute of Science and Technology of Bioethanol (INCT-Bioethanol) (FAPESP 2011/57908-6 and 2014/50884-5, CNPq 574002/2008-1 and 465319/2014-9) (Brazil), and the EPSRC via DTP EP/N509565/1.

Appendix A. Supplementary data

Supplementary data to this article can be found online at <https://doi.org/10.1016/j.foodchem.2022.134939>.

References

- Abokitse, K., Wu, M., Bergeron, H., Grosse, S., & Lau, P. C. K. (2010). Thermostable feruloyl esterase for the bioproduction of ferulic acid from triticale bran. *Applied Microbiology and Biotechnology*, 87(1), 195–203. <https://doi.org/10.1007/s00253-010-2441-6>
- Akin, D. E., Borneman, W. S., Rigsby, L. L., & Martin, S. A. (1993). p-Coumaroyl and feruloyl arabinoxylans from plant cell walls as substrates for ruminal bacteria. *Applied and Environmental Microbiology*, 59(2), 644–647. <https://doi.org/10.1128/AEM.59.2.644-647.1993>
- Barberousse, H., Roiseux, O., Robert, C., Paquot, M., Deroanne, C., & Blecker, C. (2008). Analytical methodologies for quantification of ferulic acid and its oligomers. *Journal of the Science of Food and Agriculture*, 88, 1494–1511. <https://doi.org/10.1002/jsfa.3242>
- Biely, P., Singh, S., & Puchart, V. (2016). Towards enzymatic breakdown of complex plant xylan structures: State of the art. In *Biotechnology Advances* (Vol. 34(7), pp. 1260–1274). Elsevier Inc. <https://doi.org/10.1016/j.biotechadv.2016.09.001>
- Bunzel, M., Allerding, E., Sinwell, V., Ralph, J., & Steinhart, H. (2002). Cell wall hydroxycinnamates in wild rice (*Zizania aquatica* L.) insoluble dietary fibre. *European Food Research and Technology* 2002 214:6, 214(6), 482–488. <https://doi.org/10.1007/S00217-002-0512-3>.
- Chandra, P., Enespa, Singh, R., & Arora, P. K. (2020). Microbial lipases and their industrial applications: A comprehensive review. *Microbial Cell Factories*, 19(1). <https://doi.org/10.1186/S12934-020-01428-8>
- Cochran, B., Lunday, D., & Miskevich, F. (2008). Kinetic analysis of amylase using quantitative Benedict's and iodine starch reagents. *Journal of Chemical Education*, 85(3), 401–403. <https://doi.org/10.1021/ED085P401>
- Crepin, V. F., Faulds, C. B., & Conner, I. F. (2003). Functional classification of the microbial feruloyl esterases. *Applied Microbiology and Biotechnology*, 63(6), 647–652. <https://doi.org/10.1007/S00253-003-1476-3>
- de Souza, A. P., Leite, D. C. C., Pattathil, S., Hahn, M. G., & Buckeridge, M. S. (2012). Composition and structure of sugarcane cell wall polysaccharides: implications for second-generation bioethanol production. *BioEnergy Research*, 6(2), 564–579. <https://doi.org/10.1007/S12155-012-9268-1>
- Dilokpimol, A., Mäkelä, M. R., Aguilar-Pontes, M. V., Benoit-Gelber, I., Hildén, K. S., & de Vries, R. P. (2016). Diversity of fungal feruloyl esterases: updated phylogenetic classification, properties, and industrial applications. *Biotechnology for Biofuels*, 9(1), 1–18. <https://doi.org/10.1186/S13068-016-0651-6>
- Dilokpimol, A., Mäkelä, M. R., Varriale, S., Zhou, M., Cerullo, G., Gidijala, L., ... de Vries, R. P. (2018). Fungal feruloyl esterases: Functional validation of genome mining based enzyme discovery including uncharacterized subfamilies. *New Biotechnology*, 41, 9–14. <https://doi.org/10.1016/J.NBT.2017.11.004>
- Donaghy, J. A., Bronnenmeier, K., Soto-Kelly, P. F., & McKay, A. M. (2000). Purification and characterization of an extracellular feruloyl esterase from the thermophilic anaerobe *Clostridium stercorarium*. *Journal of Applied Microbiology*, 88(3), 458–466. <https://doi.org/10.1046/J.1365-2672.2000.00983.X>
- Donaghy, J., Kelly, P. F., & McKay, A. M. (1998). Detection of ferulic acid esterase production by *Bacillus* spp. and *Lactobacilli*. *Applied Microbiology and Biotechnology*, 50(2), 257–260. <https://doi.org/10.1007/s002530051286>
- Gianfreda, L., & Scarfi, M. R. (1991). Enzyme stabilization: state of the art. *Molecular and Cellular Biochemistry*, 100.
- Goldstone, D. C., Villas-Bôas, S. G., Till, M., Kelly, W. J., Attwood, G. T., & Arcus, V. L. (2010). Structural and functional characterization of a promiscuous feruloyl esterase

- (Est 1 E) from the rumen bacterium *Butyrivibrio proteoclasticus*. *Proteins: Structure, Function and Bioinformatics*, 78(6), 1457–1469. <https://doi.org/10.1002/prot.22662>
- Grabber, J. H., John Ralph, A., & Hatfield, R. D. (1998). Ferulate cross-links limit the enzymatic degradation of synthetically lignified primary walls of maize. *Journal of Agricultural and Food Chemistry*, 46(7), 2609–2614. <https://doi.org/10.1021/JF9800099>
- Hoffmann, R. A., Leeflang, B., de Barse, M., Kamerling, J., & Vliegthart, J. (1991). Characterisation by ¹H-NMR spectroscopy of oligosaccharides, derived from arabinoxylans of white endosperm of wheat, that contain the elements -4)[alpha-L-Araf-(1-3)]-beta-D-Xylp-(1- or -4)[alpha-L-Araf-(1-2)][alpha-L-Araf-(1-3)]-beta-D-Xylp-(1-. *Carbohydrate Research*, 221(1), 63–81. [https://doi.org/10.1016/0008-6215\(91\)80049-5](https://doi.org/10.1016/0008-6215(91)80049-5)
- Jooyandeh, H., Kaur, A., & Minhas, K. S. (2009). Lipases in dairy industry: A review. *Journal of Food Science and Technology*, 46(3), 181–189.
- Kormelink, F. J. M., Hoffmann, R. A., Gruppen, H., Voragen, A. G. J., Kamerling, J. P., & Vliegthart, J. F. G. (1993). Characterisation by ¹H NMR spectroscopy of oligosaccharides derived from alkali-extractable wheat-flour arabinoxylan by digestion with endo-(1 → 4)-β-d-xylanase III from *Aspergillus awamori*. *Carbohydrate Research*, 249(2), 369–382. [https://doi.org/10.1016/0008-6215\(93\)84101-B](https://doi.org/10.1016/0008-6215(93)84101-B)
- Koseki, T., Ito, Y., Furuse, S., Ito, K., & Iwano, K. (1996). Conversion of ferulic acid into 4-vinylguaiaacol, vanillin and vanillic acid in model solutions of shochu. *Journal of Fermentation and Bioengineering*, 82(1), 46–50. [https://doi.org/10.1016/0922-338X\(96\)89453-0](https://doi.org/10.1016/0922-338X(96)89453-0)
- Kroon, P., Garcia-Conesa, M., Fillingham, I., Hazlewood, G., & Williamson, G. (1999). Release of ferulic acid dehydrodimers from plant cell walls by feruloyl esterases. *Journal of the Science of Food and Agriculture*, 79(3), 428–434. [https://doi.org/10.1002/\(sici\)1097-0010\(19990301\)79:3<428::aid-jsfa275>3.3.co;2-a](https://doi.org/10.1002/(sici)1097-0010(19990301)79:3<428::aid-jsfa275>3.3.co;2-a)
- Kumar, N., & Pruthi, V. (2014). Potential applications of ferulic acid from natural sources. *Biotechnology Reports*, 4(1), 86. <https://doi.org/10.1016/J.BTRE.2014.09.002>
- Kumari, A., Rosenkranz, T., Fitter, J., Kayastha, M., & A.. (2011). Structural stability of soybean (*Glycine max*) α-amylase: Properties of the unfolding transition studied with fluorescence and CD spectroscopy. *Protein & Peptide Letters*, 18(3), 253–260. <https://doi.org/10.2174/092986611794578305>
- Lama, L., Tramice, A., Finore, I., Anzelmo, G., Calandrelli, V., Pagnotta, E., ... Trincone, A. (2014). Degradative actions of microbial xylanolytic activities on hemicelluloses from rhizome of *Arundo donax*. *AMB Express*, 4(1), 1–9. <https://doi.org/10.1186/s13568-014-0055-6>
- Lequart, C., Nuzillard, J. M., Kurek, B., & Debeire, P. (1999). Hydrolysis of wheat bran and straw by an endoxylanase: Production and structural characterization of cinnamoyl-oligosaccharides. *Carbohydrate Research*, 319(1–4), 102–111. [https://doi.org/10.1016/S0008-6215\(99\)00110-X](https://doi.org/10.1016/S0008-6215(99)00110-X)
- Mathew, S., & Abraham, T. E. (2008). Ferulic acid: An antioxidant found naturally in plant cell walls and feruloyl esterases involved in its release and their applications. *Critical reviews in Biotechnology*, 24(2–3), 59–83. <https://doi.org/10.1080/07388550490491467>
- Nankar, R., Prabhakar, P. K., & Doble, M. (2017). Hybrid drug combination: Combination of ferulic acid and metformin as anti-diabetic therapy. *Phytomedicine*, 37(October), 10–13. <https://doi.org/10.1016/j.phymed.2017.10.015>
- Oliveira, D. M., Mota, T. R., Oliva, B., Segato, F., Marchiosi, R., Ferrarese-Filho, O., ... dos Santos, W. D. (2019). Feruloyl esterases: Biocatalysts to overcome biomass recalcitrance and for the production of bioactive compounds. *Bioresource Technology*, 278, 408–423. <https://doi.org/10.1016/j.biortech.2019.01.064>
- Ou, S., Wang, Y., Tang, S., Huang, C., & Jackson, M. G. (2005). Role of ferulic acid in preparing edible films from soy protein isolate. *Journal of Food Engineering*, 70(2), 205–210. <https://doi.org/10.1016/J.JFOODENG.2004.09.025>
- Rakotoarivonina, H., Hermant, B., Chabbert, B., Touzel, J. P., & Remond, C. (2011). A thermostable feruloyl-esterase from the hemicellulolytic bacterium *Thermobacillus xylanilyticus* releases phenolic acids from non-pretreated plant cell walls. *Applied Microbiology and Biotechnology*, 90(2), 541–552. <https://doi.org/10.1007/s00253-011-3103-z>
- Ralet, M.-C., Faulds, C. B., Williamson, G., & Thibault, J.-F. (1994). Degradation of feruloylated oligosaccharides from sugar-beet pulp and wheat bran by ferulic acid esterases from *Aspergillus niger*. *Carbohydrate Research*, 263, 257–269.
- Raveendran, S., Parameswaran, B., Ummalyma, S. B., Abraham, A., Mathew, A. K., Madhavan, A., ... Pandey, A. (2018). Applications of microbial enzymes in food industry. *Food Technology and Biotechnology*, 56(1), 16. <https://doi.org/10.17113/FTB.56.01.18.5491>
- Rémond, C., Boukari, I., Chabat, G., & O'Donohue, M. (2008). Action of a GH 51 α-l-arabinofuranosidase on wheat-derived arabinoxylans and arabinoxylooligosaccharides. *Carbohydrate Polymers*, 72(3), 424–430. <https://doi.org/10.1016/j.carbpol.2007.09.008>
- Russo, M., Marquez, A., Herrera, H., Abejin-Mukdsi, C., Saavedra, L., Hebert, E., ... Medina, R. (2020). Oral administration of *Lactobacillus fermentum* CRL1446 improves biomarkers of metabolic syndrome in mice fed a high-fat diet supplemented with wheat bran. *Food & Function*, 11(5), 3879–3894. <https://doi.org/10.1039/D0FO00730G>
- Schendel, R. R., Becker, A., Tyl, C. E., & Bunzel, M. (2015). Isolation and characterization of feruloylated arabinoxylan oligosaccharides from the perennial cereal grain intermediate wheat grass (*Thinopyrum intermedium*). *Carbohydrate Research*, 407, 16–25. <https://doi.org/10.1016/J.CARRES.2015.01.006>
- Singh, R., Kumar, M., Mittal, A., & Mehta, P. K. (2016). Microbial enzymes: Industrial progress in 21st century. 3. *Biotech*, 6(2). <https://doi.org/10.1007/S13205-016-0485-8>
- Trono, D. (2019). Recombinant enzymes in the food and pharmaceutical industries. In *Advances in Enzyme Technologies* (pp. 349–387). Elsevier Inc. <https://doi.org/10.1016/B978-0-444-64114-4.00013-3>
- van Boekel, M., Fogliano, V., Pellegrini, N., Stanton, C., Scholz, G., Lalljie, S., ... Eisenbrand, G. (2010). A review on the beneficial aspects of food processing. *Molecular Nutrition and Food Research*, 54(9), 1215–1247. <https://doi.org/10.1002/MNFR.200900608>
- van Munster, J. M., Thomas, B., Riese, M., Davis, A. L., Gray, C. J., Archer, D. B., & Flitsch, S. L. (2017). Application of carbohydrate arrays coupled with mass spectrometry to detect activity of plant-polysaccharide degradative enzymes from the fungus *Aspergillus niger*. *Scientific Reports*, 7(1), 43117. <https://doi.org/10.1038/srep43117>
- Wong, D. W. S. (2006). Feruloyl esterase. *Applied Biochemistry and Biotechnology*, 133(2), 87–112. <https://doi.org/10.1385/ABAB:133:2:87>
- Zeng, J., Tong, Z., Wang, L., Zhu, J. Y., & Ingram, L. (2014). Isolation and structural characterization of sugarcane bagasse lignin after dilute phosphoric acid plus steam explosion pretreatment and its effect on cellulose hydrolysis. *Bioresource Technology*, 154, 274–281. <https://doi.org/10.1016/J.BIORTECH.2013.12.072>